

# Quantum Carry Research of Q1D – SE on Helium at Charged Substrate

Viktor A. Nikolaenko<sup>1,\*</sup> and Sviatoslav S. Sokolov<sup>1</sup>

<sup>1</sup>*Institute for Low Temperature Physics and Engineering, National Academy of Sciences of Ukraine, Ukraine*

**Abstract:** Known in nanoelectronics a solid-state quantum size systems motivate creating like systems using the surface electrons on liquid helium. The quantum carry of quasi-one-dimensional surface electrons (Q1D-SEs) over superfluid helium is considered here. Research is conducted based on an electron phase diagram in the gas phase under conditions far from electron quantum melting. A substrate is dense row of the light guide segments where the SEs channels are formed over helium in the fiber gaps between. The electrostatic model of substrate profile demonstrates modulation of potential in the electric field leading to possibility of the fiber top charge thereby improving the Q1D-SEs channels' quality. The experiments carried out by a low-frequency electron transport method at the temperature from 1.5 K to 0.5 K and the concentrations of electrons were up to  $10^9\text{cm}^{-2}$ . The SE movement transverse to the channel satisfies quantization conditions in terms of both temperature and electron relaxation time in the system. According to the experiment, below a certain temperature, the SE conductivity is ladder-like. The differential of SE conductivity is peak-like corresponding qualitatively to an electron states density. The distance between peaks accords to the 1D energy spectrum in some approach. Possibility of applying the 1D-SEs quantized energy levels (vibration levels) as quantum bits for a quantum computer is considered.

**Keywords:** quantum well, quantum wire, superfluid helium, surface electron, quantum bit

## 1. Introduction

At the structure size of matter is comparable to the electron de Broglie wavelength, quantum effects are well expressed. Modern nano-technologies let create a clear quantum size systems (QSSs) are use for both the fundamental researches and the applied purposes. The effects of electron move quantization in the QSSs are observed at the electron energy spectrum resolution higher than temperature and at sufficient electron relaxation time in the system. As noted, metal matter does not satisfy QSS formation conditions due to both the high Fermi energy level (greater than 1 eV) and the small electron relaxation time. The semiconductor matter can be candidate to QSS. The surface electrons (SEs) either on helium layers or on others cryogenic condensed matters with smooth surface relate to the QSSs too. Due to both the low polarization of the substrate material and its negative affinity for electrons, the SEs move quasi-free over the substrate. The QSSs in nano-electronic are known as next: the quantum well; the quantum wire; the quantum dot; the heterostructure; and others [1].

The specific properties of SEs on the helium surface were noted in theoretical works [2, 3] independently. The surface electron is localized in a shallow potential well and is distant from the surface. The Fermi energy of SEs,  $\varepsilon_F = \pi \hbar^2 n_s / (2m)$  (here  $\hbar$  is Plank constant;  $n_s$  is concentration of 2D surface electrons;  $m$  is the mass of free electron) is small enough relative to temperature, so the electron system is nondegenerated. The SE movement transverse to the substrate surface is quantized with a hydrogen-like spectrum,

where  $\sim 7$  K is the ground state energy, which is higher than the temperature in the experiments. The SE mobility along the helium surface is high, and it is limited only by both the interaction electrons with helium atoms in gas and the interaction with riplons. The SE Wigner crystallization at some conditions is proof of cleanliness this system. The SE system advantages are the broad variation of both the electron density and the scatterers type in one experiment. The disadvantage of the SE system on the massive liquid helium is the limitation of the electron density near  $2 \cdot 10^9 \text{ cm}^{-2}$  on value due to an electro-hydrodynamic instability of charged surface leading to losses of the electrons either partly or full. The roughness of the solid substrate matter beneath helium layer can cause the thermo-activation carry of electrons. SEs serve both the object of study and the conducting model of solid-state matter [4]. The surface electrons can serve as sensitive chips in nanoelectronics and as quantum bits (QBs) for a quantum computer (QC), considering either the discrete electron energy levels or the electron spins [5, 6].

The periodical modulation of the substrate properties leads the dimensionality of the surface electron system to one-dimensional (1D-SEs) or lower. For creating 1D-SE system, the profiled substrate can be used. 1D-SE states on the bottom of the curved helium surface in the profiled substrate groove have been proposed and realized in works [7, 8] correspondingly. The detailed theoretical description was performed in work [9]. In last work, in particular, the quantization of the electron collision frequency as function of the 1D-SE energy spectrums is considered at both the electron-riplon interaction and the electron-He atom interaction. The narrow and clean electron stripes are need to the quantization of one-dimensional move. The

\*Corresponding author: Viktor A. Nikolaenko, Institute for Low Temperature Physics and Engineering, National Academy of Sciences of Ukraine, Ukraine. Email: [nikolaenko@ilt.kharkov.ua](mailto:nikolaenko@ilt.kharkov.ua)

influence of quantum effects on the electron carry is essential, and the simplest electron transport methods are enough for experimental research here.

The Q1D-SE quantum effects studied in this work use the gaps between cylinder light guides filled with helium. According to an electron phase diagram, the research was fulfilled in electron gas phase at the temperatures and at the surface electron concentration far from the quantum melting process.

The practical aims of many contemporary works are the theoretical and the experimental researches for creating a quantum bits on surface electrons for quantum computing [10–15]. Row of the international and national groups intensively gives attention to this problem in last decade. The leader of the scientific group, David Schuster, with collaborators (USA), and researcher Jin D, study key questions: “Coupling a single electron on superfluid helium to a superconducting resonator,” “Single electron on solid neon as a solid-state qubit platform,” and related topics. Other group is Denis Konstantinov with collaborators (Japan). Their works dedicated row themes, for example, “Observation of the Rydberg’s resonances in surface electrons over superfluid helium confined in a solid matter with 4- $\mu\text{m}$  deep channel”. Group performs much works concern to the novel devices projects and to the research of the fundamental basis for building the quantum bits over the helium or other cryogenic matters. Thus, a micro-structured device was created: a superconducting coplanar-waveguide (CPW) resonator integrated with an electron trap to study the “coupling of the SE spin states to the Rydberg states.” A separate theme is testing SE movement under both microwave radiation and the transition to Wigner crystallization. Others researches have dealt with analogical questions using cryogenic condensed matters or others as substrate, and they give some examples of qubits in practice too [16–19].

The possibility of building QBs on the quantized vibrational levels of one-dimensional surface electrons over superfluid helium, which were preliminarily considered in [20], is the focus of the present work. The works use the known basic consequences of the Schrödinger and Laplace equations to analyze the 1D electron system. In current work, the historical moment leading to the practical search 1D–SE energy levels is noted too. The bibliography is essentially supplemented here, focusing on the study and design of QBs on surface electrons over cryogenic matters.

The original substrate for QBs in the present work is a combination of micro-channels, coaxial rings with  $R$  and  $r$ , and radial channels. The UHF technique with high-quality cavity working on the  $H_{011}$  oscillation mode for QB manipulations can be applied.

The current work addresses the possibility of creating QBs for QC using the transverse oscillation of one-dimensional electrons, as discussed in item 6 of this work: “Possibility of applying 1D-SE quantization levels over superfluid helium as QBs for QC”.

Original part of paper structure consists of introduction; experimental setup; electrostatic consideration of a dielectric cylinder (light guide); experimental results; discussion; possibility apply a 1D-SEs quantization levels over superfluid helium as QBs of QC; conclusion.

## 2. Experimental Setup

Building a clear Q1D system on a semiconductor basis motivates realizing this system on a surface electron basis. The idea of the work is to create relatively narrow and stable Q1D-SEs channels by adding to the outer electric field the field of charges

is placed directly on tops of the profiled substrate. The coplanar field of charged stripes increases thereby the potential well and shifts surface electrons to the channel center apart from the groove borders. The Q1D-SE spectrum increases on value  $\omega^2 \sim \pi^2 e^2 n_x / ma^2$  (where  $e$  is the electron charge,  $n_x$  is the linear charge density on the substrate tops, and  $a$  is the interval between charges or charge groups). The value  $\hbar\omega$  can achieve the energy magnitude near 0.5 K.

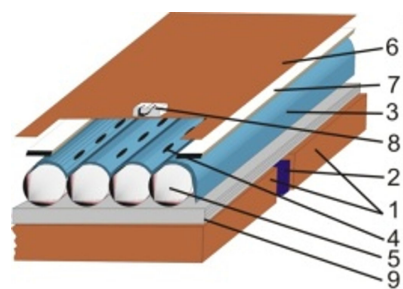
Popular in the experimental research of SEs, a low-frequency transport method is applied in this work. Conductance features of the Q1D electron system on the charged profiled substrate are investigated using the Sommer–Tanner technique [21]. Method essence is analyzing conductivity of the charged system on substrate which coupled in the capacitive manner with the coplanar capacitor plates. Some details of the measurements concerning Q1D-SE channels can be seen in work [22]. The measurements were carried out on the signal frequency 20 kHz at the value signal in range 2–150 mV rms. The temperature interval was from 1.5 K to 0.5 K, and both the 4He and 3He refrigerators were used for temperature variation.

### 2.1. Cell

The design of cell in detail is shown in Figure 1. The two neighboring plates  $5 \times 12 \text{ mm}^2$  in size (position 1) organized the measurement coplanar capacitor. Between the measurement electrodes, a screening stripe of 0.5 mm in section (position 2) functions to isolate crosstalk noise. Parallel to a measurement capacitor is situated a upper plate (position 6). The dielectric substrate with charges (position 5) is located inner to cell. Upper plate has negative potential for keeping charges on substrate with definition density. The guard ring (position 7) has negative potential and served for forming the electron spot with sharp borders.

The capacitance between parts of the measurement electrodes (position 1 in Figure 1) is up to 80 fF without surface electrons on the substrate and correspondingly with SEs on the substrate this value is much larger in magnitude. The measurement signal from generator directed to one measurement electrode and other one is connected with high sensitive two-phase lock-in analyzer. The leading electric field has been directed along conducting channels. Measurement has a current scheme model because the impedance of SEs on the substrate is much higher than the input impedance of the measurement system.

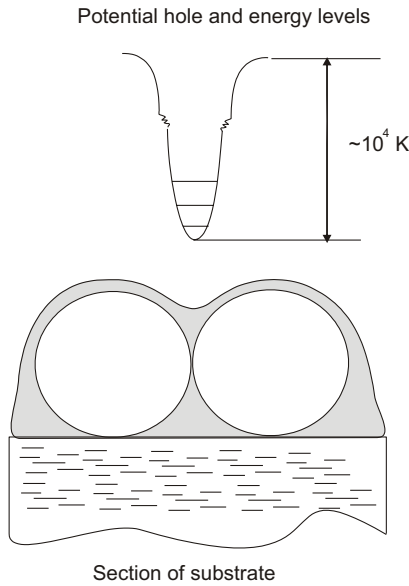
**Figure 1**  
Cell structure with a profiled substrate for forming the 1D SE system: 1 – measurement electrodes; 2 – screening stripe; 3 – helium film; 4 – 1D system of surface electrons; 5 – substrate (row of light guides); 6 – electric clamping electrode; 7 – guard ring; 8 – electron source (glow tungsten thread); 9 – insulating plate



## 2.2. Substrate

**Figure 2**

The substrate section for forming the electron one-dimensional channel over helium is shown in Figure 2: two cylinder light guide segments with curved surface of superfluid helium form the channel for SEs (bottom picture); a 1D potential well in the clamping electric field with energy levels of 1D-SE (upper picture)



The profiled substrate represents a tightly laid row of light guides in quantity 35 segments by  $100 \mu\text{m}$  in diameter situated on thin insulating plate (shown in Figure 1, positions 5 and 9). The superfluid helium flows on substrate into space between light guides creating the liquid curved grooves because of both the capillary and the gravity forces. The liquid helium curvature radius in groove depends on distance substrate over massive helium. In the presence of an applied electric field, the grooves are filled with SE lines over helium during the experimental process. In Figure 2 are shown schematically both the potential

well for SE over curved helium surface between the cylindrical fibers (Figure 2, bottom picture) and the 1D energy spectrum in potential well (Figure 2, upper picture).

Preliminarily, some experiments were performed on a substrate where, instead of light guides, nylon threads  $90 \mu\text{m}$  in diameter were used, which can charge spontaneously in an external field due to their quality.

The real fiber surface quality of light guide is different from ideal, and its roughness has been defined by an atomic force microscopy (AFM) method (Figure 3).

As can see on the AFM tracks, the roughness of the light guide surface is  $0.7 \text{ nm}$  rms in amplitude. The local inhomogeneity pikes are near  $4 \text{ nm}$  in amplitude with  $\sim 20 \mu\text{m}$  in interval. The effective electric potential variation along the conducting channel with SEs leads to the value which can express as next

$$\delta V \approx -\frac{\epsilon_d - 1}{16(\epsilon_d + 1)} \frac{e^2}{\pi \epsilon_0 Z} \frac{\pi \xi}{A} \left(\frac{A}{Z}\right)^{1/2} e^{-\frac{2\pi Z}{A}} \quad (1)$$

Here,  $\epsilon_d$  and  $\epsilon_0$  are the dielectric constant of both the substrate and the vacuum, respectively; the value  $Z$  is the distance of surface electron to substrate; value  $\xi$  is the inhomogeneities effective amplitude; and value  $A$  is the effective distance between inhomogeneities. The estimations give next: at equal the values  $A$  and  $\xi$  and when the value  $Z$  is about  $10^{-5}$ – $10^{-6}$  cm in magnitude so, the effective potential variation,  $\delta V$ , is near magnitude  $10^{-3}$  K in the channel center. This value is increasing in magnitude near edge of border.

## 2.3. Procedure

The sequence of experimental steps is implemented as follows. The nontermolized electrons from the glow tungsten thread ( $5 \mu\text{m}$  in diameter) were directed with a pressing electric field to the tops of the profiled substrate. These form charged stripes with a fixed potential (The electrostatic consideration of the possibility of charging the top of the dielectric cylindrical fiber is in item 3 below). The slow moving thermolized electrons at the additional outer field are formed conducting SE channels on helium into the substrate grooves. The substrate electron density,  $n$ , either of the surface electrons or of the charged stripes has been determined by the values the specific cell capacitance with dielectric substrate,  $C$ , and the pressing potential,  $V_{\perp}$ , namely,  $n = C \cdot V_{\perp} / e$ . This causes a shift in

**Figure 3**  
Atomic force microscopy (AFM) of the light guide surface (comment is beneath of picture)

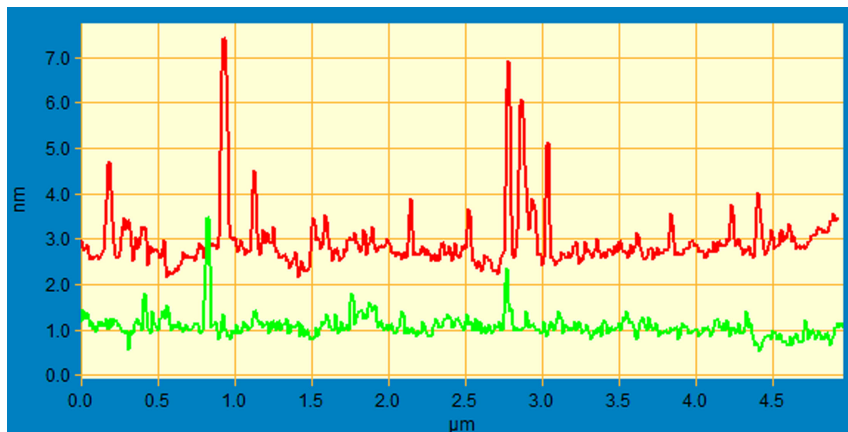
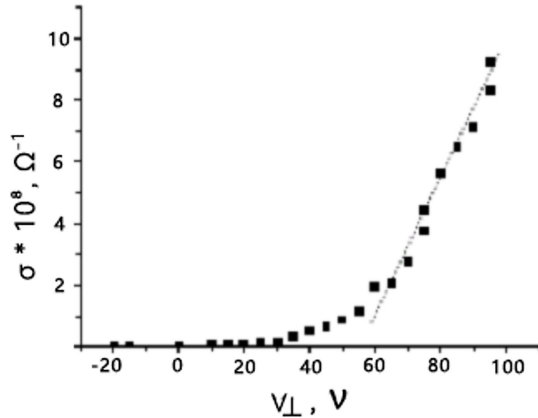


Figure 4

An example of the shift to the right in the value of  $\sigma$  vs  $V_{\perp}$  for SEs in the linear grooves of the substrate with charged stripes. According to the dependence, the potential of the charged stripes is greater than 50 V. The extrapolation line, by intersection with the potential axis, determines this value's magnitude. After that, the SE conductivity behavior,  $\sigma$ , is practically proportional to the value of  $\Delta V_{\perp}$  (where  $\Delta$  is the difference in potential values)



the conductivity dependence from  $V_{\perp}$  to the right on the potential axis, defining the charged stripes potential (Figure 4, for example).

The experiments were carried out at different electron concentrations, both the charged stripes and the surface electrons, ranging from zero electron density to the values up to  $10^9$  cm<sup>-2</sup>, accordingly. The temperature dependences of SE conductivity are considered in item 4, "Experimental results".

### 3. Electrostatic Consideration of a Dielectric Cylinder (Light Guide)

It is known that the dielectric structured substrate in a uniform electric field causes electric potential variations in the section. The analysis of the changes in electric potential  $\varphi$  and electric field  $E$  on the section of the surface dielectric cylinder top is considered here. The dielectric permittivity of the light guide is much higher than that of the surrounding space, including liquid helium. Cross-section of the cylindrical light guide in the coordinate system is shown in Figure 5.

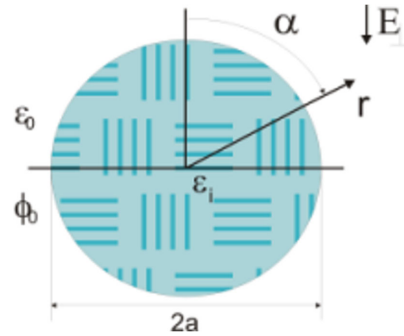
In the cylindrical coordinate system  $(r, \alpha)$ , the Laplace equation under both conditions—the perpendicular uniform electric field and the uncharged substrate—is  $\Delta\varphi = 0$  (where  $\Delta$  is the Laplace operator and  $\varphi$  is the electric potential of the dielectric cylinder). The variations of the electric potential along the cylinder axis in this coordinate system are absent, i.e.,  $d\varphi/dz = 0$ . Take to account Fourier's replacement for  $\varphi$  as  $\varphi = M(r) \cdot N(\alpha)$  the Laplace's equation transform to next expression with a separating variables  $r$  and  $\alpha$ .

$$\frac{r}{M} \frac{d}{dr} \left( r \cdot \frac{dM}{dr} \right) + \frac{1}{N} \frac{d^2 N}{d\alpha^2} = 0 \quad (2)$$

The appropriate adjustment constants in the solution of each separate term in the full expression are based on the equality of both the electric potentials and the normal components of electric induction at the cylinder border. According to solution of equation, the electric field either inside cylinder or near the cylinder border top or bottom, respectively, is

Figure 5

Cross-section of the cylindrical light guide in the cylindrical coordinate system: picture for electrostatic consideration. Here,  $r$  and  $\alpha$  are radial and axial coordinates, respectively; value  $\varphi_0$  is the electric field potential outside the dielectric cylinder; values  $\epsilon_0$  and  $\epsilon_i$  are dielectric permittivity outside and inside cylinder respectively



$$E_i = E_{\perp} \frac{2\epsilon_i}{\epsilon_i + \epsilon_e} \quad (3)$$

Here value  $\epsilon$  is the dielectric permittivity of corresponding matter; symbols  $e$  and  $i$  are indices of the permittivity values outside and inside of cylinder, accordingly. The value of potential near cylinder border,  $\varphi_e$  is

$$\varphi_e = E_{\perp} \left[ \left( \frac{\epsilon_i - \epsilon_e}{\epsilon_i + \epsilon_e} \right) \cdot \frac{a^2}{r} - r \right] \cdot \cos \alpha + \varphi_0 \quad (4)$$

To summarize the electrostatic consideration of a dielectric cylinder, the following points should be noted:

- The intensity of electric field inside dielectric cylinder (and near top surface) is twice more than outside cylinder at large dielectric constant of cylinder relative to surrounding matter (see expression (3));
- Function  $[\cos]$  is even so the electric potential is a parabolic function on  $\alpha$  near a top cylinder border (see expression (4));
- Here arises the possibility directly of the dielectric cylinder's tops acquiring a linear charge due to the parabolic potential well across the cylinder.

### 4. Experimental Results

The calibration dependence of Q1D-SE conductivity  $\sigma$  on temperature  $T$ , without the charge stripes on the substrate, is shown in Figure 6, which compares the result with other analogous dependencies at different potential values for both the SEs and the charged profiled substrate. As can be seen in Figure 6, the dependence  $\sigma$  from  $T$  is smooth. The dependence is strongly increasing, more order, at decreasing temperature from 1.3 K to 0.8 K (regime interaction surface electrons with He atoms in gas phase). From 0.8 K to 0.5 K (preferential interaction surface electrons with ripples on helium surface, helium gas go to freeze), this dependence is practically independent temperature. The mobility of SEs for the broad Q1D channel over liquid helium was considered early for these regimes. The mobility of SEs in the ripplon scattering region is  $\mu_r = 8a\hbar/emE_{\perp}^2$  (here

Figure 6

The temperature dependence of conductivity  $\sigma$  of quasi-one-dimensional surface electrons, in the absence of charge stripe potential on the profiled substrate, is formed by light guides

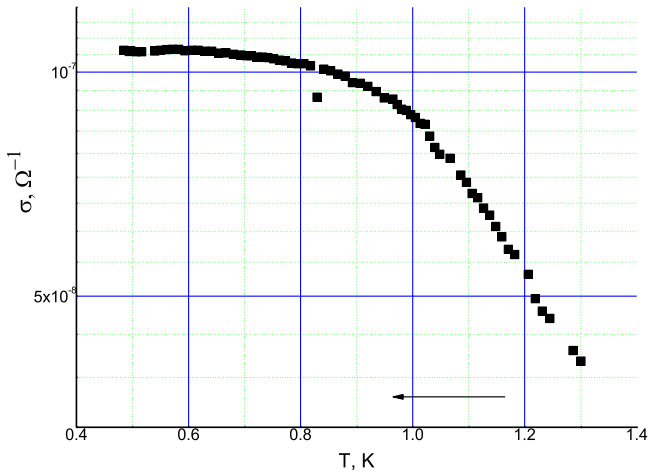
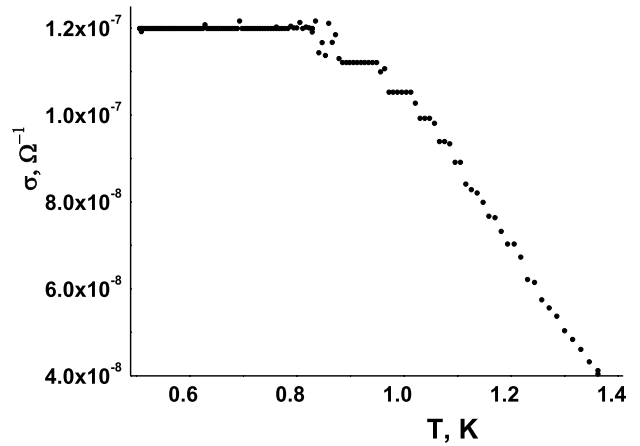


Figure 8

Temperature dependence of Q1D-SE conductivity,  $\sigma$ , in channels at small stripe charge (beginning research with stripes charge on the light guide tops)



value  $\alpha$  is the helium surface tension coefficient). The mobility of SEs in the helium gas scattering region is  $\mu_g = 8e / (3\pi\hbar\sigma_p n_g \gamma)$  (here  $\sigma_p$  is the section scattering of electron on the helium atom in gas;  $\gamma^{-1} \sim 8$  nm is the Borh's radius for surface electron over helium;  $n_g$  is helium gas density).

The research results, including the corresponding temperature dependencies of conductivity at various substrate charge potentials and SE potentials, are shown below in Figures 7–12.

Before working with the regular substrate (light guides on a dielectric plate), as noted above (item 2.2, Substrate), separate research was performed with nylon threads on a glass plate, which can charge spontaneously due to the low quality of the nylon threads. Some irregular conductivity, with small jumps, was observed at temperatures below 1 K (Figure 7).

Figure 7

Temperature dependence conductivity of a Q1D-SE at spontaneity charged substrate with nylon threads on glass plate. This is the first observation of irregularities  $\sigma$  vs  $T$  dependence. In the temperature range between 1.0 K and 0.83 K, irregularities of small jumps occur

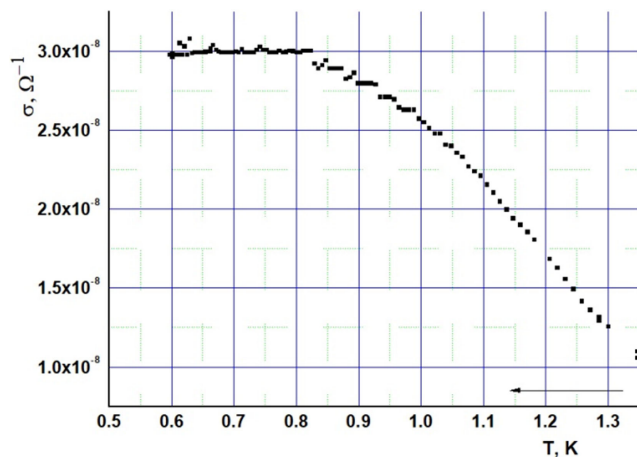


Figure 9

$\sigma$  vs  $T$  dependence of Q1D-SEs is measured at the substrate charge potential,  $V$ , approximately 5 V: upper curve is obtained at cooling cell from 1.5 K to 0.5 K at the start of this research and under curve takes a place at an increasing temperature of cell from 0.5 K to 1.52 K in same experimental process

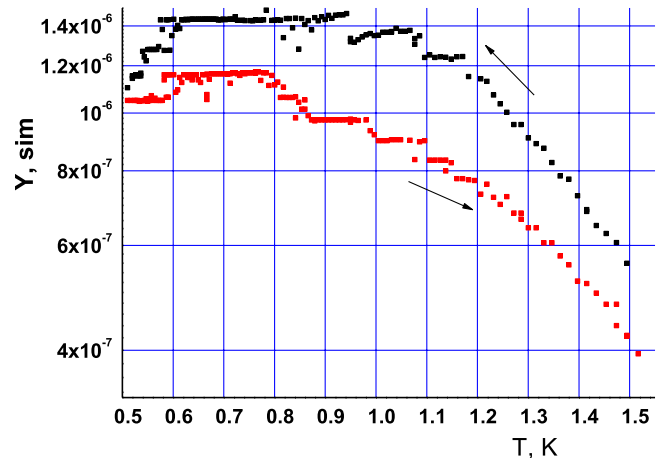


Figure 7 presents the experimental investigation of irregularities in conductivity as a function of temperature, previously performed using nylon threads (90  $\mu$ m in diameter) on a glass plate as the profiled substrate. It is shown the temperature dependence conductivity of Q1D-SE at spontaneity charged substrate and have a place the irregularities in temperature range between 1.0–0.83 K as small jumps.

Figure 8 shows the exponential dependence of Q1D-SE conductivity in the temperature range from 1.4 K to 0.8 K, which is due to scattering of electrons with He atoms in the gas (the He gas region). The ripplon scattering regime occurs at  $T < 0.8$  K. But here, a ladder-like pattern of conductivity occurs in the temperature interval below 1.1 K. This feature is due to the quantization of Q1D-SE motion, the steps become more pronounced as the temperature decreases. Last can be explained



Figure 10

Dependence conductivity,  $\sigma$ , of Q1D-SEs from  $T$  at high electron concentrations; both the SEs and the stripes charge: the upper conductivity dependence, curve 1, was measured at electron densities near  $5.4 \cdot 10^8 \text{ cm}^{-2}$  (here is left axis for conductivity) and the under conductivity dependence, curve 2, was measured at the electron densities  $\sim 10^9 \text{ cm}^{-2}$  (here is right axis of the conductivity) respectively. The cycling passages on  $T$  practically does not change this dependence

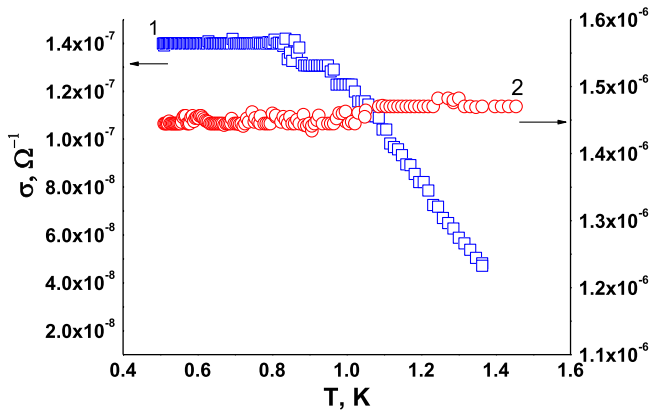
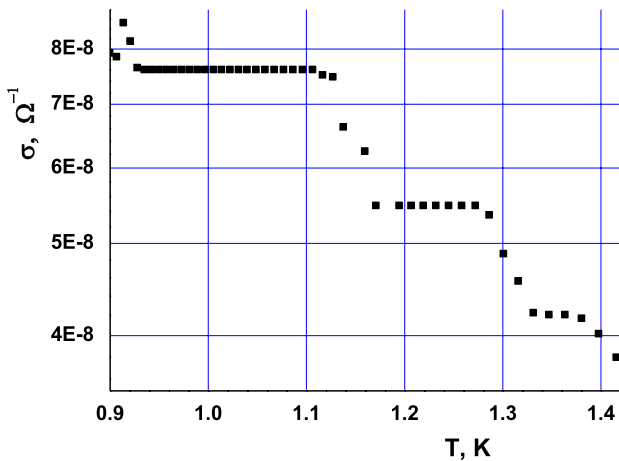


Figure 11

The temperature dependence of Q1D-SEs conductivity,  $\sigma$ , after row of the cycling passages on  $T$ . Here, the potentials 15 V have a place for both the charged stripes and the SEs

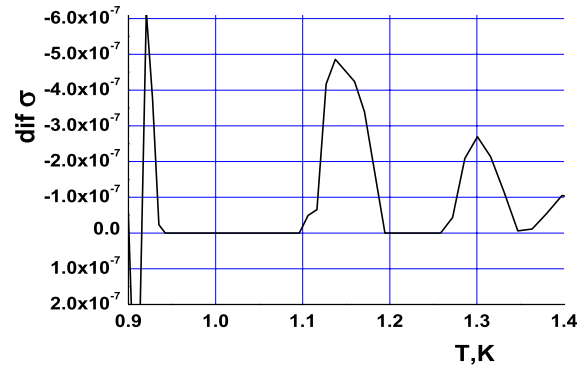


by the increase in immobile SEs with decreasing  $T$  near some roughness of the channel border, due to the thermo-activation effect. The part of immobile SE increases 1D potential well and shifts mobile SE to the channel center.

Initially, a substrate with insufficient glass surface quality was used to obtain the temperature dependencies of conductivity (Figure 9). The upper arrow of Figure 9 indicates the lowering temperature at start of the experiment and under arrow and lower curve related to increasing temperature (return move) in this experiment. At temperature lower 1.2 K, the conductivity ladder-like steps have a place on both curves but more clean steps demonstrates the bottom curve. It is supposed that there is a

Figure 12

Differential temperature dependence of Q1D-SEs conductivity which given in Figure 11



tendency to the redistribution of electrons along each stripe over time relative to the previous dependence.

At high electron densities, both the SEs and the stripe charge the temperature dependence Q1D-SE conductivity are shown in Figure 10. Here, curve 1 shows the conductivity dependence at electron densities near  $5.4 \times 10^8 \text{ cm}^{-2}$  during the cooling of the experimental cell. Curve 2 shows the conductivity dependence at electron densities  $\sim 10^9 \text{ cm}^{-2}$  during cell heating. It can be seen in Figure 10 that the maximum of the quantization step in conductivity occurs 0.5 K approximately (curve 2), which corresponds to a 3 cm range of radiation oscillations. So the 3 cm technique can be used for spectroscopic study and manipulations in this case.

Figures 11 and 12 demonstrate the temperature dependence of Q1D-SEs conductivity and the differential of that value in temperature interval 0.9 – 1.4 K for high-quality substrate (after cleaning). The results are obtained after a series of temperature cycles. The SEs potential and the stripe charge potential have values 15 V. It can be seen in Figure 11 that the dependence  $\sigma$  vs  $T$  is well expressed as a ladder-like pattern, with steps increasing as the temperature decreases. The differential value exhibits a peak-like character (Figure 12), which qualitatively coincides with the electron states density.

Summing up the experimental results need notice next. The substrate charge is used for improving the SE channels' quality by increasing 1D potential well. The SE quantization move is manifested itself as the conductivity ladder-like dependence from temperature. The duration of the steps depends on the electron densities of both the Q1D-SEs potential and the substrate electron charges. Steps duration varied in researches from zero (without the substrate charge, Figure 6) to near 0.5 K in value (Figure 10, curve 2). The energy intervals of Q1D-SE spectrum accord to the steps duration, and the differential of the conductivity temperature dependence (Figure 12) is qualitatively coinciding with the electron states density.

## 5. Discussion

As stated above, the effects of electron motion quantization in QSSs are observed when the energy spectrum resolution of the electron,  $\Delta\epsilon$ , exceeds the temperature  $T$ , and when the electron relaxation time in the system,  $\tau$ , is sufficient, i.e.,  $\epsilon_{n+1} - \epsilon_n > k_B T$  and  $\epsilon_{n+1} - \epsilon_n > \hbar/\tau$ . According to solution of stationary

Schrodinger's equation for 1D surface electron at the parabolic potential,  $U(y) = m\omega_0^2 y^2/2$ , the wave function of basic electron state is

$$\psi(y) = \pi^{-1/4} y_0^{-1/2} \exp\left(-\frac{y^2}{2y_0^2}\right) \quad (5)$$

Value  $y_0^2 = \hbar/(2\pi m\omega_0)$  is the SE localization length square to cross-channel.

The harmonic spectrum size of a 1D electron system corresponding to frequency,  $\omega_0$ , in potential well (see Figure 2) is

$$\omega_0^2 = e \cdot E_{\perp} / (m \cdot R) \quad (6)$$

The value  $R = \sigma' / (\rho \cdot g \cdot h)$  is the curvature radius of liquid helium surface in groove (here  $\sigma$  is the surface tension of superfluid helium and  $\rho$  is the helium density; value  $g$  is gravity constant) which in experiments takes a place 35  $\mu\text{m}$  in size. The energy spectrum of one-dimensional electron at parabolic potential is

$$\varepsilon = (n + 1/2) \cdot \hbar \cdot \omega_0 + \hbar^2 \cdot k_x^2 / 2m \quad (7)$$

Value  $k_x$  is the wave vector of an electron along conducting channel.

The depth of 1D potential well over helium in groove of profiled substrate can estimate as  $\varphi \sim e \cdot E \cdot \delta$  (here value  $\delta$  is a deflection the liquid surface from horizon in groove).

Notably, estimates according to [8] give the following magnitudes:  $\varphi \sim 10^4$  K;  $\hbar\omega_0 \sim 0.1$  K; and  $y_0 \sim 30$  nm, at a clamping electric field of  $4.5 \times 10^4$  V/m in magnitude. As considered above, the linear charges on the stripe tops shift the Q1D-SE inter-energy lines of the spectrum, and the magnitude of this value can exceed 0.5 K.

The inhomogeneities have a place on profiled substrate in spite of cleaning one (Figure 3), that leads to the thermo-activation carry of electrons. According to Arrhenius law, the conductivity of channels is expressed as  $\sigma = \sigma_0 \exp \Delta/T$  (here  $\Delta$  is energy of thermo-activation;  $\sigma_0$  is the conductivity of clean channels). The effective magnitude of value  $\Delta$  in most experiments was near 1 K.

Thus, the number of immobile electrons near the boundary increases with decreasing  $T$ , and they can contribute to the linear electron charge on the structured substrate, thereby increasing the potential well for SE.

## 6. Possibility of Applying a 1D-SEs Quantization Levels over Superfluid Helium as QBs of QC

Researchers Platzman and Dykman considered the possibility of creating a QC using two-dimensional surface electrons (2DSEs) over superfluid helium, with a periodic set of governing electrodes [5]. The basic energy level and the first excited energy level of SE as quantum bit (QB) were proposed to use. Both the SE Rydberg levels and their Stark shift by the electric field according to the outer microwave energy are considered. The Wigner's crystallization of SEs leads to the entanglement of electron states. The quantum ionization of the excited electrons into the free space through adjustable potential barrier for reading out the electron states is proposed.

In our original work, we consider the possibility of building QBs using the transverse vibration energy levels of one-dimensional electrons over liquid helium (schematic of energy levels shown similarly in Figure 2, upper part). The above investigations of quantized motion in Q1D-SE form the basis for considering that proposition. The substrate is a combination of micro-channels with cross-sectional value  $\delta$ , arranged as coaxial rings with radii  $R$  and  $r$ , connected by identical radial channels

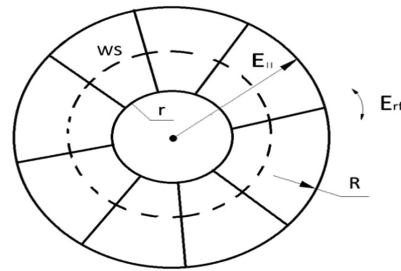
(Figure 13). The SE can move along radial channel between rings by the radial directed electric field. The substrate can be situated in a cylinder superconductivity UHF cavity with high-quality factor of the  $H_{011}$  mode.

Over the nodes of the large-radius ring, in the applied vertically electric field, 1D-SEs vibration energy levels  $\hbar\omega_0$  are formed, with the wave functions of the ground state as shown in (5). The frequency of equidistant spectrum,  $\omega_0$ , is shown in (7). The quantized vibration states of surface electron are considered as a qubit basis. The Q1D-SE superposition state of QB can be defined by both the Rabi's frequency pulse and the Stark shift is caused by pulse electric field. The Rabi Frequency is

$$\Omega = \frac{eE_{rf} \langle 0 | y | 1 \rangle}{\hbar} \quad (8)$$

$E_{rf}$  is intensity of Rabi electric field and cause the transition of SE between the vibration energy levels  $\langle 0 \rangle$  and  $\langle 1 \rangle$ .

**Figure 13**  
Combination of 1D micro-channels for QBs of QC: the coaxial micro-channel rings with large,  $R$ , and small,  $r$ , radii are connected each other the radial micro-channels



The entanglement of the electron states occurs at the Wigner crystallization of SEs (indicated by the dashed line in Figure 13), which is manifested in the corresponding ratio of the potential energy from Coulomb interaction between electrons to the kinetic energy, specifically the thermodynamic one, namely:

$$e^2(\pi \cdot n_s)^{1/2} / (4 \cdot \pi \cdot \varepsilon \cdot \varepsilon_0 \cdot k_B \cdot Tc) = \Gamma. \quad (9)$$

where  $\Gamma^{-1} = 1/137.035$  is constant of the thin structure,  $k = 1.38 \cdot 10^{-23}$  J/K is the Boltzmann's constant,  $\varepsilon$  and  $\varepsilon_0$  are dielectric permittivity of the substrate and the vacuum, respectively.

As noted, in the current research (Figure 10, curve 2), the energy quantization level 0.5 K in magnitude can be achieved in Q1D-SE vibration spectra, and the 3 cm technique can be considered for QB manipulation.

Readout of the Q1D-SE state after reverse moving can be detected either by the micro-capacity or by the SET (single electron transistor). Estimates can be next. The radius magnitudes are  $R \sim 1$  mm and  $r \sim 0.1$  mm accordingly;  $\delta \sim 1-2$   $\mu\text{m}$ ; the UHF cavity  $H_{011}$  resonance is 9.4 GHz (the 3 cm technique), where value  $\Delta\varepsilon = \hbar \cdot \omega_0$  is  $\sim 0.5$  K. Near a small diameter ring, the electron crystal goes to melt at temperature near 20 mK. The surface electron quantity can achieve value  $5 \cdot 10^2$  over nodes and that can be the QC scale. It must be noted that the quality of cavity with superconducting coating (Sn matter, e.g.) can achieve  $10^{10}$  and more in magnitude.

## 7. Conclusion

Summarizing it must be noted next. Study quantum carry features of quasi-one-dimensional surface electrons over superfluid helium on a charged substrate reveals energy levels that can be applied to building quantum bits. According to the idea, the charge of a profiled substrate can essentially improve the SEs conducting channels by increasing the 1D potential well. The researches were performed in the electron gas phase.

The substrate profile in the electrostatic model, according to Laplace's equation under both conditions of a perpendicular uniform electric field and an uncharged substrate, demonstrates modulation of potential, allowing for the charging of the substrate tops. The experimental profiled substrate consists of a row of cylindrical light guide segments, 100  $\mu\text{m}$  in diameter, tightly laid on an insulating plate. The superfluid helium flows onto the substrate, filling the space between light guides and creating liquid curved grooves, due by both capillary and gravity forces. In the experiment, the grooves are filled with SE lines over helium.

The low-frequency electron transport method, commonly used to study low-dimensional surface electrons, was applied here. The ladder-similar dependence  $\sigma$  vs  $T$  in experiment was displayed on profiled substrate using the light guides. The step picture depends on the electron density both the Q1D-SEs and the substrate charge. The steps can vary from zero (without the substrate charge, Figure 6) to near 0.5 K in value (Figure 10). The energy intervals of Q1D-SE spectrum accord to the ladder's steps duration as supposed. The differential of the surface electron conductivity dependence on temperature is peak-like and qualitatively corresponds to the electron states density. The conductivity steps don't depend on the measurement signal parameters, but they depend on the substrate surface quality. The experimental investigation of conductivity irregularities as a function of temperature was previously performed using a profiled substrate with nylon threads 90  $\mu\text{m}$  in diameter. It was shown (Figure 7), the temperature dependence of Q1D-SEs conductivity on a spontaneously charged substrate of low quality exhibits irregularities. In temperature range between 1.0 K – 0.83 K is observed a small jumps.

More pronounced stairs in the conductivity as temperature decreases can be explained by both electron redistribution to lower energy levels in the Q1D system and the increasing number of immobile electrons near the channel boundary, according to Arrhenius's law. The experimental investigation coincides with theoretical consideration at some approximation.

It is possible to apply the 1D-SEs quantization levels for building QBs, and the 3 cm technique can be used for QB manipulations. QB state can govern both the electric field pulses and the UHF pulses. Designed set of 1D micro-channels is arranged as coaxial rings with  $R$  (outer) and  $r$  (inner) radii which connected each other analogical radial channels (Figure 13). The SEs can move on channels between rings via a radially directed electric field, and entanglement of SE states is possible at electron Wigner crystallization in the space between rings.

In recent works [23, 24], it was shown that electrons floating in a vacuum above the surface of liquid helium or solid neon emerge as promising candidates for qubits. Charge qubit consisting of a single electron bound to solid neon surface exhibits an exceptionally long coherence time. By evaluating the surface charges induced by the electron, its strong perpendicular binding to the neon surface was demonstrated. The Schrodinger equation for the electron's lateral motion on the curved 2D surface is then solved at extensive topographical variations. The results reveal that surface bumps can naturally bind an electron, forming unique ring-shaped quantum

states. It is shown that the electron excitation energy can be smoothly tuned using a magnetic field to facilitate qubit operation. Both the theoretical proposals and the recent experiments were also considered, primarily focusing on the use of the spin state as the qubit, wherein the spin and charge states are hybridized. Throughout these proposals and experiments, the charge state is coupled to an LC resonator, which facilitates both the control and readout mechanisms for the spin state via an artificially introduced spin-charge coupling.

It should be noted that other cryogenic solid matters with convenient quantum characteristics, with or without a helium film, can be used as substrates instead of helium and neon, such as  $\text{H}_2$ ,  $\text{D}_2$ , Kr, and others. For the neon substrate, the quantum values are the binding energy of the electron with the substrate,  $E_{\text{bin}} = 17.5$  meV, and the Bohr radius,  $\gamma^{-1} = 19$   $\text{\AA}$ , respectively. For the solid hydrogen substrate the binding energy of the electron with the substrate is  $E_{\text{bin}} = 16.7$  meV and the Bohr radius is 17  $\text{\AA}$ , respectively, and for the solid deuterium  $E_{\text{bin}} = 22$  meV and  $\gamma^{-1}$  is  $\sim 15$   $\text{\AA}$ , respectively.

Recently, a silicon spin qubit processor was proposed in work [25]. Compact 3D microwave dielectric resonators were considered as a way to deliver the magnetic fields to spin qubit control across an entire quantum chip using only a single microwave source. Here take a place "coherent Rabi oscillations of the single electron spin qubits in a planar SiMOS quantum dot device at using a global magnetic field generated off-chip".

## Ethical Statement

This study does not contain any studies with human or animal subjects performed by any of the authors.

## Conflicts of Interest

The authors declare that they have no conflicts of interest to this work.

## Data Availability Statement

Data sharing is not applicable to this article as no new data were created or analyzed in this study.

## Author Contribution Statement

**Viktor A. Nikolaenko:** Conceptualization, Methodology, Investigation, Resources, Writing – original draft, Writing – review & editing, Visualization. **Sviatoslav S. Sokolov:** Software, Validation, Formal analysis, Data curation, Writing – review & editing, Visualization, Supervision, Project administration.

## References

- [1] Alferov, Z. I. (1998). The history and future of semiconductor heterostructures. *Semiconductors*, 32, 1–14. <https://doi.org/10.1134/1.1187350>
- [2] Cole, M. W., & Cohen, M. H. (1969). Image-potential-induced surface bands in insulators. *Physical Review Letters*, 23(21), 1238. <https://doi.org/10.1103/PhysRevLett.23.1238>
- [3] Shikin, V. B. (1970). About moving of the helium ions near boundary vapor-liquid. *JETPH*, 58, 1748.
- [4] Monarkha, Y., & Kono, K. (2004). *Two-dimensional Coulomb liquids and solids*. Germany: Springer.



- [5] Platzman, P. M., & Dykman, M. I. (1999). Quantum computing with electrons floating on liquid helium. *Science*, 284(5422), 1967–1969. <https://doi.org/10.1126/science.284.5422.1967>
- [6] Lyon, S. A. (2006). Spin-based quantum computing using electrons on liquid helium. *Physical Review A—Atomic, Molecular, and Optical Physics*, 74(5), 052338. <https://doi.org/10.1103/PhysRevA.74.052338>
- [7] Kovdrya, Y. Z., & Monarkha, Y. P. (1986). One-dimensional electron system over liquid helium. *Fizika Nizkikh Temperatur*, 12(10), 1011–1015.
- [8] Kovdrya, Y. Z. (2003). One-dimensional and zero-dimensional electron systems on liquid helium. *Low Temperature Physics*, 29(2), 77–104. <https://doi.org/10.1063/1.1542406>
- [9] Sokolov, S. S., Hai, G. Q., & Studart, N. (1995). Mobility of electrons in a quasi-one-dimensional conducting channel on the liquid-helium surface. *Physical Review B*, 51(9), 5977. <https://doi.org/10.1103/PhysRevB.51.5977>
- [10] Koolstra, G., Yang, G., & Schuster, D. I. (2019). Coupling a single electron on superfluid helium to a superconducting resonator. *Nature Communications*, 10(1), 5323. <https://doi.org/10.1038/s41467-019-13335-7>
- [11] Zhou, X., Koolstra, G., Zhang, X., Yang, G., Han, X., Dizdar, B., . . . , & Jin, D. (2022). Single electrons on solid neon as a solid-state qubit platform. *Nature*, 605(7908), 46–50. <https://doi.org/10.1038/s41586-022-04539-x>
- [12] Kawakami, E., Elarabi, A., & Konstantinov, D. (2021). Relaxation of the excited Rydberg states of surface electrons on liquid helium. *Physical Review Letters*, 126(10), 106802. <https://doi.org/10.1103/PhysRevLett.126.106802>
- [13] Zou, S., Konstantinov, D., & Rees, D. G. (2021). Dynamical ordering in a two-dimensional electron crystal confined in a narrow channel geometry. *Physical Review B*, 104(4), 045427. <https://doi.org/10.1103/PhysRevB.104.045427>
- [14] Zou, S., Grossenbach, S., & Konstantinov, D. (2022). Observation of the Rydberg resonance in surface electrons on superfluid helium confined in a 4- $\mu\text{m}$  deep channel. *Journal of Low Temperature Physics*, 208(3), 211–222. <https://doi.org/10.48550/arXiv.2201.05351>
- [15] Jin, D. (2020). Quantum electronics and optics at the interface of solid neon and superfluid helium. *Quantum Science and Technology*, 5(3), 035003. <https://doi.org/10.1088/2058-9565/ab8695>
- [16] Chatterjee, A., Stevenson, P., De Franceschi, S., Morello, A., de Leon, N. P., & Kuemmeth, F. (2021). Semiconductor qubits in practice. *Nature Reviews Physics*, 3(3), 157–177. <https://doi.org/10.1038/s42254-021-00283-9>
- [17] Chen, S., Raha, M., Phenicie, C. M., Ourari, S., & Thompson, J. D. (2020). Parallel single-shot measurement and coherent control of solid-state spins below the diffraction limit. *Science*, 370(6516), 592–595. <https://doi.org/10.1126/science.abc7821>
- [18] Wolfowicz, G., Heremans, F. J., Anderson, C. P., Kanai, S., Seo, H., Gali, A., . . . , & Awschalom, D. D. (2021). Quantum guidelines for solid-state spin defects. *Nature Reviews Materials*, 6(10), 906–925. <https://doi.org/10.1038/s41578-021-00306-y>
- [19] Krantz, P., Kjaergaard, M., Yan, F., Orlando, T. P., Gustavsson, S., & Oliver, W. D. (2019). A quantum engineer's guide to superconducting qubits. *Applied Physics Reviews*, 6(2), 021318. <https://doi.org/10.1063/1.5089550>
- [20] Nikolaenko, V. A., Smorodin, A. V., & Sokolov, S. S. (2021). Quantization conductivity of surface electrons over superfluid helium at the charged substrate channels. In *2021 IEEE 11th International Conference Nanomaterials: Applications & Properties*, 1–4. <https://doi.org/10.1109/NAP51885.2021.9568517>
- [21] Sommer, W. T., & Tanner, D. J. (1971). Mobility of electrons on the surface of liquid  $^4\text{He}$ . *Physical Review Letters*, 27(20), 1345. <https://doi.org/10.1103/PhysRevLett.27.1345>
- [22] Gladchenko, S. P., Nikolaenko, V. A., Kovdrya, Y. Z., & Sokolov, S. S. (2001). Carrier transport and localization in a one-dimensional electronic system over liquid helium. *Low Temperature Physics*, 27(1), 1–9. <https://doi.org/10.1063/1.1344136>
- [23] Kanai, T., Jin, D., & Guo, W. (2024). Single-electron qubits based on quantum ring states on solid neon surface. *Physical Review Letters*, 132(25), 250603. <https://doi.org/10.1103/PhysRevLett.132.250603>
- [24] Jennings, A., Zhou, X., Grytsenko, I., & Kawakami, E. (2024). Quantum computing using floating electrons on cryogenic substrates: Potential and challenges. *Applied Physics Letters*, 124(12), 120501. <https://doi.org/10.1063/5.0179700>
- [25] Vahapoglu, E., Slack-Smith, J. P., Leon, R. C., Lim, W. H., Hudson, F. E., Day, T., . . . , & Pla, J. J. (2022). Coherent control of electron spin qubits in silicon using a global field. *npj Quantum Information*, 8(1), 126. <https://doi.org/10.1038/s41534-022-00645-w>

**How to Cite:** Nikolaenko, V. A., & Sokolov, S. S. (2024). Quantum Carry Research of Q1D – SE on Helium at Charged Substrate. *Journal of Optics and Photonics Research*. <https://doi.org/10.47852/bonviewJOPR42023430>